ChemComm

One-pot synthesis of nanocaterpillar structures via in situ nanoparticlization of fully conjugated poly(p-phenylene)-block-polythiophene

Journal:	*ChemComm*
Manuscript ID:	CC-COM-04-2014-002787.R1
Article Type:	Communication
Date Submitted by the Author:	30-May-2014
Complete List of Authors:	Choi, Tae-Lim; Seoul National University, Lee, In-Hwan; Seoul National University, Chemisty Amaladass, Pitchamuthu; Seoul National University, Chemisty

Journal Name

COMMUNICATION

One-pot synthesis of nanocaterpillar structures via in situ nanoparticlization of fully conjugated poly(*p*-phenylene)-*block*-polythiophene

In-Hwan Lee, Pitchamuthu Amaladass and Tae-Lim Choi*

1D nanocaterpillar structures were spontaneously formed during the synthesis of fully conjugated poly(2,5-dihexyloxy-1,4-phenylene)-*block*-polythiophene due to the strong π-π interactions between the polythiophene blocks. With the elongation of the polythiophene block, nanostructures evolved from nanospheres to nanocaterpillars, and their length and height increased with good control.

Self-assembly of conjugated polymers has been investigated intensively as a way to produce well-ordered semiconducting materials with intriguing nanostructures and optoelectronic properties.[1] For example, block copolymers based on polythiophene derivatives have self-assembled into a wide range of nanostructures such as nanospheres,[2] nanowires,[3a-i] helical nanowires,[3c] nanorings,[3b] and vesicles,[4] and these nanostructures are promising materials in optoelectronic applications.[5] However, to induce the formation of these well-defined nanostructures from block copolymers, post-synthetic processes such as aging, changing the temperature, and the addition of selective solvents and additives are required to promote crystallization-driven self-assembly, as there is no sufficient driving force for the self-assembly of block copolymers during their syntheses.

To prepare various nanostructures consisted of conjugated polymers by a simple and direct method during synthesis, our group developed a one-pot process called in situ nanoparticlization of conjugated polymers (INCP).[6] This process is based on a (quasi) living polymerization that produces diblock copolymers with soluble polymers as the first block and completely insoluble conjugated polymers as the second block. During the polymerization, these conjugated polymers spontaneously create highly stable nanostructures by forming a well-defined core as a result of the strong π-π interactions or solvophobic effect of the second block. For example, INCP with soluble polynorbornene as the first block and polyacetylene as the insoluble second block (PN-*b*-PA) formed
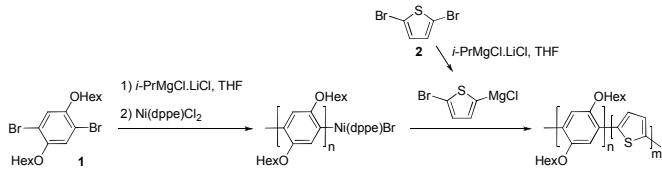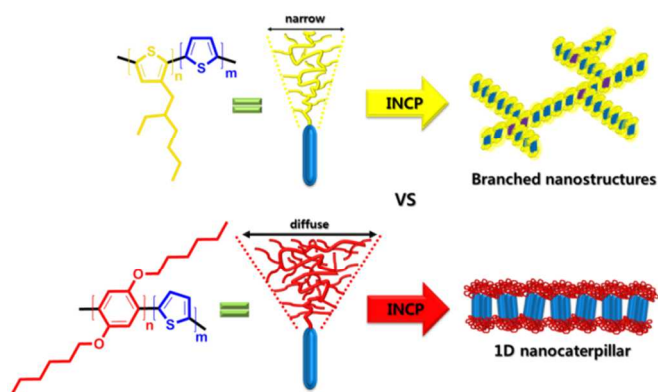
Scheme 1. INCP schemes for (a) P3EHT-*b*-PT (highly exposed cores are depicted in purple)[6c] versus (b) PPP-*b*-PT

one-dimensional (1D) nanocaterpillar structures.[6a] However, INCP of PN-*b*-PA produced virtually insulated 1D nanostructures because of the non-conjugated backbone of the polynorbornene shell. In order to solve this problem, we performed INCP with fully conjugated poly(3-(2-ethylhexyl)thiophene)-*block*-polythiophene (P3EHT-*b*-PT), which self-assembled into highly branched hierarchical nanostructures such as nanostars and nanonetworks.[6c] Although the formation of unique nanostructures from the fully conjugated polymer itself was interesting, we could not control their shape to produce 1D nanostructures, which would be more useful in electronic applications. We reasoned that the P3EHT shell was too rigid, so that the shell covering the insoluble PT core was not effective enough, thereby producing branched nanostructures. In this Communication, we report the formation of 1D nanocaterpillar structures by INCP of fully conjugated poly(2,5-dihexyloxy-1,4-phenylene)-*block*-polythiophene (PPP-*b*-PT). Because the PPP shell has a larger hydrodynamic volume than the previously used P3EHT

shell, this new block copolymer produced well-defined and stable 1D nanostructures with good control over the length (Scheme 1).

In order to prepare well-defined 1D nanostructures, we designed a new block copolymer where the first block (or shell) has a larger hydrodynamic volume than P3EHT. PPP was a good candidate, not only because it contains two hexyl side chains extending in opposite directions per repeat unit, but also because the polymer backbone of PPP was twisted with a higher dihedral angle than P3EHT.[7] These factors could provide improved stability of the nanostructures[8] and better solubility or covering ability of the PPP shell toward the solvophobic PT core. Because controlling the exposure of the core is crucial for determining the type of nanostructure formed in the INCP process,[6a,c] this feature of PPP may prevent premature exposure of the core which leads to highly branched nanostructures from P3EHT-*b*-PT, and result in the formation of 1D nanostructure.

Table 1. Synthesis of PPP-*b*-PT by the GRIM method

entry	Ni(dppe)Cl$_2$:**1**:**2**	M_n (PDI) of PPP[a]	DP of PT[b]	yield
1	1:70:30	9.9k (1.26)	14	39%
2	1:70:55	10.4k (1.26)	37	51%
3	1:70:70	12.5k (1.35)	56	61%
4	1:70:90	10.1k (1.16)	76	42%

[a]Measured by THF size exclusion chromatography calibrated using polystyrene standards. [b]Estimated by gas chromatography-mass spectrometry.

To test this idea, various PPP-*b*-PTs were prepared by a quasi-living Grignard metathesis (GRIM) method.[9] The catalyst loading of (1,2-bis(diphenylphosphino)ethane)dichloronickel(II) (Ni(dppe)Cl$_2$) was 1.45 mol% with respect to monomer **1** in all cases, and the **2**/Ni(dppe)Cl$_2$ ratio was varied from 30:1 to 90:1 (Table 1). The number average molecular weight (M_n) and polydispersity index (PDI) of the first block (PPP) were approximately 10 kg/mol and 1.2–1.3, respectively, and the degree of polymerization (DP) of the PT block increased linearly with the equivalents of monomer **2** (Table 1). These results suggested that GRIM polymerization of PPP-*b*-PTs was well controlled. These PPP-*b*-PTs were soluble in organic solvents such as chloroform and chlorobenzene.

The first evidence of successful self-assembly via INCP of the PPP-*b*-PTs was obtained from ^{1}H and ^{13}C NMR analyses, which showed identical spectra for the PPP homopolymer and the PPP-*b*-PTs; in other words, the signals for the second block (PT) were absent (Figure S1). This was a characteristic feature of INCP, and it suggested that the PPP-*b*-PTs assembled into core-shell type nanostructures in which the PT block formed the highly aggregated core as a result of strong π-π interactions.[6]

Next, observation of the color change during synthesis and the UV-vis spectral features of the final polymers provided insightful information about the block copolymer synthesis and in situ nanostructure formation. When the Grignard reagent from monomer **2** was added to the reaction flask containing PPP with a living chain end, the color of the solution quickly changed from yellow to red, and finally to dark purple within 2 minutes. UV-vis analysis of the final products in chloroform disclosed some structural details on the

block copolymer, showing two absorbance peaks, one corresponding to the that of a PPP homopolymer (absorbance maximum (λ_{max}) at 340 nm and onset point at 370 nm) and the other corresponding to that of PT (a broad absorption from 370 to 640 nm). This absorption from the PT block showed two distinct vibronic peaks at 556 and 598 nm, which indicated strong π-π interactions even in solution, and their intensities increased along with an increase in the DP of PT. In addition, their onset points gradually increased from 625 to 637 nm (E_g = 2.0 eV) (Figure 1). The UV-vis spectra of the PPP-*b*-PTs in the film state showed similar absorption spectra as in solution (Figure S2 (a)). Moreover, UV-vis spectra of the film after thermal annealing at 150 °C and 200 °C for 10 min showed no significant changes when compared to those of the solution and the pristine film (Figure S2 (a)–(e)). These observations indicated that the PT core of the resulting nanostructures without any post-treatment were highly ordered and well stacked even in solution.
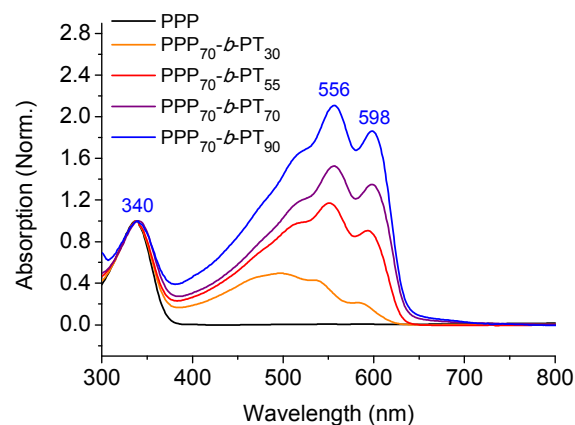

Fig. 1 UV-vis spectra of PPP-*b*-PT in chloroform at room temperature

Further details on the crystallinity of the diblock copolymers in the solid state were investigated by powder X-ray diffraction (PXRD) and differential scanning calorimetry (DSC) analyses. PXRD of PPP-*b*-PTs showed two distinct peaks, the (100) reflection of PPP with a *d*-spacing of 2.1 nm and a broad peak with a *d*-spacing of 0.38–0.44 nm corresponding to the (110) and (200) reflections of PT as well as the (010) and (001) reflections of PPP (Figure S3).[10] The intensity of the (110) and (200) peaks from PT gradually increased with an increase in the DP of PT, from 14 to 76, implying that the crystallinity of the PT core was enhanced along with its increasing DP (Figure S3). This agreed with the UV-vis analysis showing the increased vibronic peaks with the increasing DP of PT. The melting temperature (T_m) and crystallization temperature (T_c) of the PPP-*b*-PTs were approximately 85 °C (based on the second DSC scan) and approximately 40 °C (based on the first DSC scan), respectively, reflecting the thermal transition of the PPP block (Figure S4 (c)–(h)). The melting enthalpy (ΔH_m) gradually decreased from 34 to 9 J/g with the increase in the DP of PT, because restricted geometry of the core-shell structures would loosen the packing of the PPP block (Figure S4 (h)). On the other hand, T_m related with PT block was not observed in the DSC scan (from 20 to 250 °C) (Figure S4 (d)–(g)).
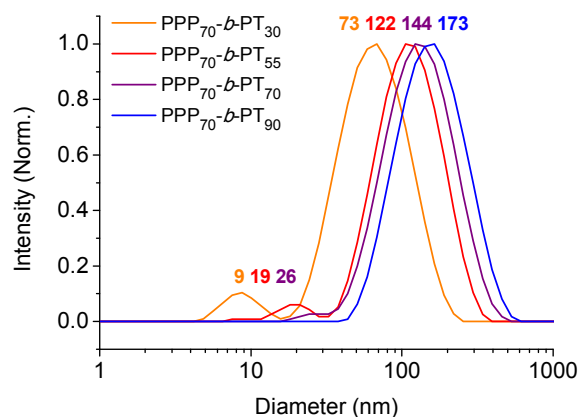
Fig 2. DLS profiles of nanocrystals from PPP-*b*-PT in chloroform at 20 °C

Detailed information on the size and shape of the nanostructures was obtained by dynamic light scattering (DLS) and imaging techniques such as atomic force microscopy (AFM) and transmission electron microscopy (TEM). At first, DLS measurements showed that the hydrodynamic diameter (D_h) of the nanoparticles in chloroform gradually increased from 73 to 173 nm with the increase in the DP of the PT block (Figure 2). In line with this increasing D_h of the nanostructures, the AFM images of the nanostructures on highly ordered pyrolytic graphite (HOPG) vividly showed a similar trend of the size increment, accompanied by a structural transformation from nanospheres to nanorods. AFM images of PPP$_{70}$-*b*-PT$_{30}$ (DP of PT = 14) showed a mixture of nanospheres and short nanorods with an average height of 4.4 nm (Figure 3(a), S5(a), and S7). With the increase in the DP of the PT core, these nanospheres and short nanorods transformed into longer nanorods (Figure 3(b)–(d) and S5(b)–(d)). The number average length (L_n) of the nanorods measured by AFM increased from 76 to 102 and further to 121 nm in accordance with the increase of the DP of PT from 37 to 56 to 76, respectively (Figure 3 and S6). The length dispersity (L_w/L_n) values of these nanorods were quite narrow (1.13–1.25) (Figure 3 and S6), even though the formation of nanorod structures via INCP follows a step-growth type supramolecular polymerization mechanism.[6a,c] The average height of the nanostructures in the AFM images gradually increased from 4.4 to 6.8 nm with the increasing DP of PT from 14 to 76, indicating that core expansion of the nanostructures was responsible for the structural evolution (Figure 3 and S7). A closer look at the nanorods by high-resolution AFM images revealed undulating nanostructures resembling a caterpillar (nanocaterpillar) (Figure 4(a), S5(c), and S8). In order to confirm the nanocaterpillar structures, we carried out TEM imaging to visualize the crystalline core part of the nanostructures. Firstly, the TEM images of the PPP-*b*-PTs showed the same nanorod structures as previously observed in the AFM images (Figure S5 (a)–(d)). More importantly, the magnified images of the crystalline core revealed that each nanorod was actually composed of nanospheres that barely touched one another (Figure 4(b)), and this suggested that the assembly of individual nanospheres was responsible for the formation of the nanocaterpillar structure.[6a,c]

Based on the various analyses presented above, we propose a similar INCP mechanism for the nanocaterpillar structure that was described in our previous reports.[6a] Briefly, PPP-*b*-PT initially starts to self-assemble into nanospheres. As the DP of PT increases, the core expands, and larger area of the solvophobic PT is exposed to
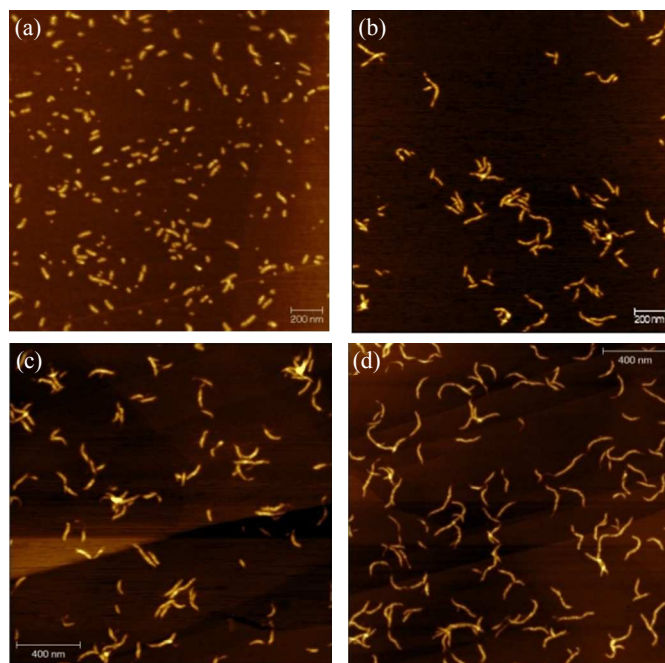
	PPP$_{70}$-*b*-PT$_{55}$	PPP$_{70}$-*b*-PT$_{70}$	PPP$_{70}$-*b*-PT$_{90}$
L_n (L_w/L_n)	76 nm (1.13)	102 nm (1.25)	121 nm (1.16)
height	5.3 nm	6.4 nm	6.8 nm

Fig. 3 AFM images of the nanostructures from PPP-*b*-PT on HOPG: (a) PPP$_{70}$-*b*-PT$_{30}$, (b) PPP$_{70}$-*b*-PT$_{55}$, (c) PPP$_{70}$-*b*-PT$_{70}$, and (d) PPP$_{70}$-*b*-PT$_{90}$
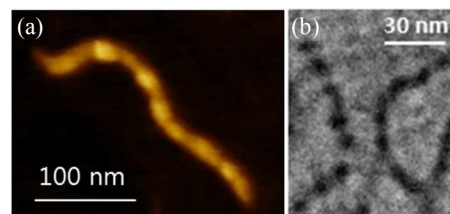

Fig. 4 Nanocaterpillar structures from PPP-*b*-PT confirmed by (a) high-resolution AFM imaging and (b) magnified TEM imaging

the solvent. To minimize this unfavorable solvation, the nanospheres with exposed cores would cling to each other by strong π-π interactions, thereby forming the nanocaterpillar structures. We believe that uncontrolled branching did not occur because the PPP shell effectively solvates the expanded PT core (Scheme 1).

Compared to the previous INCP of PN-*b*-PA, which also produced 1D nanocaterpillars, the new nanocaterpillars containing the fully conjugated PPP (shell) and PT (core) would be not only more attractive for optoelectronic materials, but was also a more uniform and well-defined 1D nanostructure with lower dispersity in length. In addition, the average length of the nanocaterpillar could be controlled by controlling the DP of PT. We attribute this to the living polymerization by GRIM, which produces PT cores with a more narrow size distribution than the ring-opening metathesis polymerization of cyclooctatetraene, in which chain transfer reactions extensively occur.

Lastly, the stability of these nanostructures toward high temperature and mechanical force (sonication) was examined. Heating the solution of PPP-*b*-PTs in chlorobenzene (or toluene) to

80 °C or sonicating the solution of PPP-*b*-PTs in chlorobenzene (or chloroform) for 4 h did not significantly change the DLS profiles (maintaining D_h), UV-vis spectra (maintaining vibronic peaks), and AFM images (maintaining their morphology) (Figure S9). This is in contrast to other 1D nanofibers consisting of conjugated polymers, which are normally unstable toward external stimuli.[3d,h] In addition, the highest occupied molecular orbital (HOMO) energy level of these nanostructures measured by cyclic voltammetry was -5.5 eV, which is lower than the HOMO of P3EHT (-5.3 eV),[6c] indicating that these nanostructures would be more stable against oxidation (Figure S10).

In conclusion, we have demonstrated the synthesis of highly stable 1D nanocaterpillar crystals from fully conjugated PPP-*b*-PTs via INCP. With an increase in the DP of PT, the morphology of the nanostructures evolved from nanospheres to nanocaterpillar structures, and the length of the nanocaterpillar could also be controlled. These nanocrystals may find potential applications as optoelectronic materials because of their well-defined structure and high stability. The formation of other nanocrystals via INCP consisting of conjugated block copolymers is currently being explored.

Notes and references

Department of Chemistry, Seoul National University, Seoul, 151-747, Korea. E-mail: tlc@snu.ac.kr

† Electronic Supplementary Information (ESI) available: Experimental details and further characterizations. See DOI: 10.1039/c000000x/

1 (a) D. Tuncel and H. V. Demir, *Nanoscale*, 2010, **2**, 484; (b) J. Pecher and S. Mecking, *Chem. Rev.*, 2010, **110**, 6260; (c) F. S. Kim, G. Ren and S. A. Jenekhe, *Chem. Mater.*, 2011, **23**, 682.

2 Z. C. Li, R. J. Ono, Z. Q. Wu and C. W. Bielawski, *Chem. Commun.*, 2011, **47**, 197.

3 (a) P.-T. Wu, G. Ren, C. Li, R. Mezzenga and S. A. Jenekhe, *Macromolecules*, 2009, **42**, 2317; (b) M. He, L. Zhao, J. Wang, W. Han, Y. Yang, F. Qiu and Z. Lin, *ACS Nano*, 2010, **4**, 3241; (c) E. Lee, B. Hammer, J.-K. Kim, Z. Page, T. Emrick and R. C. Hayward, *J. Am. Chem. Soc.*, 2011, **133**, 10390; (d) S. K. Patra, R. Ahmed, G. R. Whittell, D. J. Lunn, E. L. Dunphy, M. A. Winnik and I. Manners, *J. Am. Chem. Soc.*, 2011, **133**, 8842; (e) A. G. Hammer, F. A. Bokel, R. C. Hayward and T. Emrick, *Chem. Mater.*, 2011, **23**, 4250; (f) J. B. Gilroy, D. J. Lunn, S. K. Patra, G. R. Whittell, M. A. Winnik and I. Manners, *Macromolecules*, 2012, **45**, 5806; (g) A. C. Kamps, M. Fryd and S.-J. Park, *ACS Nano*, 2012, **6**, 2844; (h) J. Gwyther, J. B. Gilroy, P. A. Rupar, D. J. Lunn, E. Kynaston, S. K. Patra, G. R. Whittell, M. A. Winnik and I. Manners, *Chem.-Eur. J.* 2013, **19**, 9186; (i) J. Qian, X. Li, D. J. Lunn, J. Gwyther, Z. M. Hudson, E. Kynaston, P. A. Rupar, M. A. Winnik and I. Manners, *J. Am. Chem. Soc.*, 2014, **136**, 4121.

4 J. Kim, I. Y. Song and T. Park, *Chem. Commun.*, 2011, **47**, 4697.

5 (a) U. Scherf, A. Gutacker and N. Koenen, *Acc. Chem. Res.*, 2008, **41**, 1086; (b) H. Xin, F. S. Kim and S. A. Jenekhe, *J. Am. Chem. Soc.*, 2008, **130**, 5424; (c) H. Xin, G. Ren, F. S. Kim and S. A. Jenekhe, *Chem. Mater.*, 2008, **20**, 6199; (d) L. Li, G. Lu and X. Yang, *J. Mater. Chem.*, 2008, **18**, 1984; (e) J. S. Kim, J. H. Lee, J. H.

Park, C. Shim, M. Sim and K. Cho, *Adv. Funct. Mater.*, 2011, **21**, 480; (f) T. Higashihara and M. Ueda, *Macromol. Res.*, 2013, **21**, 257.

6 (a) K.-Y. Yoon, I.-H. Lee, K. O. Kim, J. Jang, E. Lee and T.-L. Choi, *J. Am. Chem. Soc.*, 2012, **134**, 14291; (b) J. Kim, E.-H. Kang and T.-L. Choi, *ACS Macro Letters*, 2012, **1**, 1090; (c) I.-H. Lee, P. Amaladass, K.-Y. Yoon, S. Shin, Y.-J. Kim, I. Kim, E. Lee and T.-L. Choi, *J. Am. Chem. Soc.*, 2013, **135**, 17695.

7 (a) K. C. Park, L. R. Dodd, K. Levon and T. K. Kwei, *Macromolecules*, 1996, **29**, 7149; (b) A. J. Berresheim, M. Müller and K. Müllen, *Chem. Rev.*, 1999, **99**, 1747; (c) Y. Zhang, K. Tajima and K. Hashimoto, *Macromolecules*, 2009, **42**, 7008.

8 (a) A. Edwards, S. Blumstengel, I. Sokolik, H. Yun, Y. Okamoto and Dorsinville, R., *Synth. Met.*, 1997, **84**, 639; (b) P. B. Balanda, M. B. Ramey and J. R. Reynolds, *Macromolecules*, 1999, **32**, 3970.

9 (a) R. Miyakoshi, K. Shimono, A. Yokoyama and T. Yokozawa, *J. Am. Chem. Soc.*, 2006, **128**, 16012; (b) R. Miyakoshi, A. Yokoyama and T. Yokozawa, *Chem. Lett.*, 2008, **37**, 1022; (c) S. Wu, L. Bu, L. Huang, X. Yu, Y. Han, Y. Geng and F. Wang, *Polymer*, 2009, **50**, 6245.

10 (a) Z. Mo, K.-B. Lee, Y. B. Moon, M. Kobayashi, A. J. Heeger and F. Wudl, *Macromolecules*, 1985, **18**, 1972; (b) H. Yang, L. Wang, J. Zhang, X. Yu, Y. Geng and Y. Han, *Macromol. Chem. Phys.*, 2014, **215**, 405.

(Table Of Contents)